

1 **SUPPLEMENTAL MATERIAL**

2 **Expanded Materials & Methods**

3 **Study design**

4 In this study, we provide genetic evidence to demonstrate that AH of *TTNtv* DCM
5 can be recapitulated in both embryonic and adult zebrafish in vivo models. And loss-
6 of-function of *ttn* is sufficient to trigger DCM-like phenotypes while *ulk1a* inhibition is
7 a therapeutic avenue. We use similar age and similar body weight *ttn* mutant lines of
8 zebrafish to compare the DCM-like phenotypes, male and female fish are equally
9 included in the research and randomly allocated into different groups, and WT fish
10 are obtained from the genotyping of *ttn* mutant in-crossing lines. Fish with unhealthy
11 conditions or slim bodies are excluded from the analysis. Power analysis was
12 performed by using PASS 11 software to determine approximate sample sizes for
13 the animal heart function analysis(1). For all animal experiments, the animal groups
14 were randomized, and the researchers were blind to the genotypes and treatments
15 of animals.

16 **Quantification of cardiac function via video imaging at the embryonic stage**

17 Zebrafish larvae at the embryonic 2 days post-fertilization (dpf) stage was
18 anesthetized with 0.02% tricaine (Argent Chemical Laboratories) for 2 minutes,
19 placed lateral side up, and held in place with 3% methylcellulose (Sigma-Aldrich).
20 The beating hearts were documented by using a Zeiss Axioplan 2 microscope with a
21 differential interference camera (DIC) lens at 10X magnification, and video clips were

22 then used to calculate the heart rates and fraction shortening (FS) using the formula
23 $[FS=(Ld-Ls)/Ld]$. FS was analyzed by using ImageJ software. Ld and Ls represent
24 the length of the short axis of the ventricle at the end-diastolic stage and end-systolic
25 stage, respectively.(2)

26 **Immunofluorescence staining of embryonic hearts and somites**

27 Embryonic hearts at 2 dpf were dissected by using two BD U-100 insulin syringes
28 and were transferred to slides with a 10 μ l pipette.(3) Dissected heart tissues and the
29 whole larvae bodies were immediately fixed with 4% PBS-buffered formaldehyde
30 (PFA) for 20 min at room temperature, permeabilized with 0.5% Triton X-100 in PBS
31 (PBST), blocked with 10% normal sheep serum/ PBST for 1 h, and incubated with
32 primary antibodies [anti-myosin heavy chain (1:50, DSHB, F59), anti- β -catenin
33 (1:200, Sigma, #C7207), anti-MEF2(A+C) (1:200, Abcam, #197070)], anti- α -
34 actinin(1:200, Sigma #A7811), anti-GFP(1:200, Abcam, #13970), anti-LAMP1(1:200,
35 Cell Signaling Technology, #15665) at 4°C overnight and then wash in PBST for 3
36 times. The hearts were then incubated with secondary antibodies [(Alexa Fluor anti-
37 mouse 488, 1:400; Invitrogen), (Alexa Fluor anti-rabbit 568, 1:400; Invitrogen)] by
38 shaking at RT for 30 mins, washed with PBST 3 times at room temperature, and
39 transferred to a slide that was pre-applied with a mounting medium with DAPI
40 (Vector, H-1200). Slides were covered and images were taken by using a Zeiss
41 Axioplan 2 microscope equipped with Apotome (Carl Zeiss).

42 **Quantification of cardiac function using echocardiography in adult zebrafish**

43 Adult fish cardiac function was measured and analyzed by using a Vevo 3100
44 imaging system equipped with a 50 MHz linear array sensor (Fujifilm Visual Sonics).
45 Gel (Aquasonic® 100, Parker Laboratories) was spread evenly over the contact
46 surface of the transducer to provide adequate coupling to the zebrafish ventral plane.
47 Adult zebrafish were anesthetized with tricaine (0.02%) for 5 minutes and placed
48 ventral side up in a homemade grooved sponge for fixation. A 50 MHz (MX700)
49 transducer was placed over the ventral side of the zebrafish and slowly panned
50 cephalad to capture an image of the sagittal imaging plane of the heart. B-mode
51 images are acquired by capturing images at the borders of the heart where the
52 sharpest is maximized. Quantification of images was performed using VevoLAB
53 workstation. Acquire and process data as described in a recent report.(4) Cardiac
54 function is quantified by calculating ejection fraction (EF) [$EF=(EDV-ESV)/EDV$] or
55 fractional shortening (FS) [$FS=(Ld-Ls)/Ld$], where EDV and ESV are end-diastolic
56 and end-systole ventricular volume, respectively. Ventricular dimensions were
57 normalized from B-mode images using body weights, i.e. EDV/body weight (BW) and
58 ESV/BW.(5)

59 **Quantitative RT-PCR**

60 Ventricles of heart tissues from adult zebrafish were harvested, tissues were
61 homogenized using a Bullet Blender tissue homogenizer (Next Advance Inc.), and
62 total RNA was extracted using TRIzol (Sigma-Aldrich) according to the
63 manufacturer's instructions. 500 ng isolated total RNA was used to generate cDNAs
64 using the Superscript III First-Strand Synthesis System (Invitrogen). Quantitative RT-

65 PCR was carried out in 96-well qPCR plates (Applied Biosystems). qPCR primer
66 pairs (*nppa*, *nppb*, *vmhcl*, *vmhc*, *ulk1a*, *ulk1b*) are listed in Table S1. Gene
67 expression was normalized to the expression level of *gapdh* using $2^{-\Delta\Delta Ct}$ (cycle
68 threshold) values. Each measurement contained at least three biological replicates.

69 **Swimming tunnel assay**

70 The swimming capacity of adult fish was analyzed by using our reported protocol,(6)
71 which was derived from previous reports.(7, 8) All fish were fasted for 24 hours prior
72 to the first swimming ability measurement. Groups of 10 adult fishes were placed into
73 a swimming tunnel spirometer (Mini Swim 170, Loligo Systems) with an initial water
74 velocity of 9 cm/s and acclimation for 20 min. The water flow was then increased in
75 stages at a rate of 8.66 cm/sec (T_i) every 150 seconds (T_{ii}) until all fish were
76 exhausted and pressed against the baffle at the end of the tunnel by the current.
77 Record the water flow velocities for the final and penultimate stages, U_i and U_{ii} ,
78 respectively. The formula for critical swimming ability (U_{crit}) is as follows:
79 $U_{crit} = U_i + [U_{ii} \times (T_i / T_{ii})]$.(9) U_{crit} was then normalized to the body length (BL). The
80 same batch of fish was tested after 1 and 2 days for validation.

81 **Histological staining of adult hearts**

82 All zebrafish heart tissues were harvested from 3-month adult fish under a Leica
83 microscope. After fish were euthanized by 0.05% tricaine for 10 min. The whole
84 hearts were dissected and were immediately fixed with 4% PFA and sent to the
85 Mayo Clinic Histology Core Facility for subsequent sample procession and paraffin

86 embedding. All histology experiments were performed using paraffin sections cut on
87 a microtome (Leica) and pre-heated on 37 °C overnight. Hematoxylin and eosin
88 (H&E) staining was then processed under standardized procedure. The density of
89 the trabecular muscle was quantified using ImageJ software.

90 **Optical Clearing of Adult Zebrafish Heart and Whole-Mount Immunostaining**

91 After fixation and permeabilization, the hearts were cleared with X-CLARITY (Logos
92 Biosystems) according to the manufacturer's instructions.(10) Briefly, the hearts
93 were incubated in hydrogel mixture [0.0025 g X-CLARITY Polymerization Initiator / 1
94 ml X-CLARITY Hydrogel Solution] overnight at 4°C, transferred to the X-CLARITY™
95 Polymerization System (Logos Biosystems C20001) with pre-setting vacuum -90
96 kpa, 37 °C for 3 hours, and was placed on a 37°C shaker for 3 days with tissue
97 clearing clearing solution [8g Sodium Dodecyl Sulfate, 1.25g Boric Acid, H₂O
98 /100ml, pH 8.4, filter with 2µm filter]. The samples were then washed in PBS
99 overnight at room temperature and sequentially incubated with the following
100 antibodies: anti-Troponin T (Sigma-Aldrich, T6277), Alexa Fluor anti-mouse IgG 488
101 (Invitrogen). Each antibody was incubated with samples for 2-3 days on a 37°C
102 shaker at a dilution of 1:200 in 6% BSA in PBS, 0.2% Triton X-100, and 0.01%
103 sodium azide. The samples were mounted with X-CLARITY Mounting Solution
104 (Logos Biosystems, # C13101). Images were acquired by using a Zeiss LSM 780
105 microscope and Zen software (Carl Zeiss Microscopy).

106 **Ultrastructural analysis**

107 Adult fish hearts for ultrastructural analysis were properly dissected out and fixed in
108 Trump's fixative solution (4% paraformaldehyde and 1% glutaraldehyde in 0.1 M
109 phosphate buffer [pH 7.2]) at room temperature for 1 hour, followed by overnight
110 incubation at 4°C. Fixed samples were subsequently processed and imaged at the
111 Mayo Clinic Electron Microscopy Core Facility using a Philips JEOL 1400+
112 transmission electron microscope.(11)

113 **MMEJ-based single guide RNA design and F0 injection**

114 Sequences for genes of interest were acquired and downloaded from the Ensemble
115 (<http://useast.ensembl.org/index.html>). Preferred exons were uploaded to an online
116 algorithm, MENTHU (<http://genesculpt.org/menthu/>) for selecting guide RNA. sgRNA
117 sequences are listed in Figure 4A and Table S2. Single guide RNAs (sgRNAs) with
118 appropriate chemical modifications were synthesized and obtained from Synthego
119 (Synthego Corporation). sgRNAs were dissolved in nuclease-free duplex buffer
120 (Integrated DNA Technologies, 11-01-03-01). 100 µM sgRNAs were used as stock
121 solutions, which were diluted to 5 µM or 10 µM as working solutions. The Alt-R Cas9
122 protein (Integrated DNA Technologies, 1081058) was diluted to 3.3 µg/µL in buffer
123 (20 mM HEPES, 100 mM NaCl, 5 mM MgCl₂, 0.1 mM EDTA at pH 7.5). Final
124 concentration of 5 µM sgRNA and 300 ng Cas9 protein were then mixed and
125 incubated in a 37°C water bath for 10 min to assemble the sgRNA-Cas9 protein
126 (sgRNP) complex. ~3 nL of the sgRNP complex with 0.01% phenol red indicator was
127 then injected into one-cell stage fish embryos to obtain F0 MMEJ injected embryos.

128 **Knockout (KO) score calculation**

129 Either individual embryos injected with an MMEJ sgRNP or tail fin from adult fish was
130 collected for extracting genomic DNA (HotSHOT method).(12) 2 μ L of resultant
131 genomic DNA lysates were used as templates for PCR analysis to quantify KO score
132 for each predicted MMEJ sgRNA. The PCR primer sequence information for KO
133 score quantification is listed in Table S1. To quantify the score, 5 μ L PCR product
134 was digested with Exonuclease I (New England Biolabs, M0293) for enzymic
135 purification and subsequently sent for Sanger sequencing at Genewiz
136 (<https://clims4.genewiz.com/CustomHome/Index>). The chromatograms from two
137 PCR amplicons using either predicted MMEJ sgRNA injected or uninjected
138 embryonic genomic DNA lysates as templates were analyzed for KO score
139 calculation using the Inference of CRISPR Edits (ICE) v2 CRISPR Analysis Tool by
140 TIDE (<https://www.synthego.com/products/bioinformatics/crispr-analysis>).(13) Percent
141 microhomology allele was calculated by dividing the KO score for the predicted
142 microhomology indel by the total KO score.

143 **Generation of stable mutants**

144 The F0-MMEJ injected mutant fish were raised to adulthood and outcrossed. The
145 individual F1 adults were tested individually via sequencing the targeted genomic
146 loci. Selected F1 containing the desirable mutations were outcrossed for 1-3
147 generations, aiming to eliminate potential off-target effects. A high-percentage (4%-
148 6%) agarose gel-based method is then used for genotyping and detecting the small

149 CRISPR-Cas9 induced indels.(14) After loading the samples into each lane, power
150 supply was set to 100 V, running time should be 2 hours. Gel images were acquired
151 using a gel-documentation system (Analytik Jena US UVP UVsolo Touch).

152 **SDS agarose gel electrophoresis**

153 Protein samples from the single zebrafish larvae were extracted by homogenization
154 using a mortar and pestle (Thermo Fisher Scientific) on the surface of dry ice.

155 Protein lysates are then moved to 30 μ l sample buffer [8 M urea, 3% SDS, 2 M
156 Thiourea, 0.05 M Tris-HCl (pH 8.0), 0.03% Bromophenol Blue, 75 mM DTT and
157 0.01% protease inhibitors cocktail (Roche)]. After the samples were incubated at
158 65°C for 15 min and then be placed on ice for 2 mins. 0.5 μ l Benzonase enzyme
159 (Sigma Chemical Company #E1014-5KU) was added to digest the genomic DNA
160 and to reduce viscosity, and then centrifuged at 4°C 12000 rpm for 10 min. The
161 supernatants were separated on a 1.2% agarose gel [0.6g SeaKem Gold Agarose
162 (Lonza #50512) heated in 10 mL 5x TGS buffer (0.25M Tris, 1.92M glycine, 2M
163 SDS) and 27 mL dH₂O, mixed with 15 mL 99.5% glycerol and keep at 65°C till use]
164 using a vertical agarose gel electrophoresis system;(15) 1 kb Plus DNA Ladder
165 (Invitrogen) was used as size markers. The gel was fixed in a prefixing solution [50%
166 methanol, 12% glacial acetic acid, 5% glycerol] for 20 mins, washed with water for
167 30 mins, dried in an oven at 50°C overnight, transferred to fixing solution [50%
168 methanol, 10% glacial acetic acid, 10% Fixative Enhancer Concentrate (Bio-Rad,
169 #1610461)], and visualized by a Silver Stain Plus Kit (Bio-Rad, #1610449).

170 **Coomassie blue staining**

171 A 2 dpf larvae were transferred to RIPA buffer (Sigma-Aldrich) and homogenized
172 using a Bullet Blender tissue homogenizer (Next Advance). The resulting protein
173 lysates were resolved on a mini-protein TGX precast gel, followed by Coomassie
174 blue staining using a standard protocol.(11)

175 **Western blotting**

176 Hearts dissected from adult fish were transferred immediately to RIPA buffer (Sigma-
177 Aldrich) supplemented with protease inhibitor cocktail (Roche), 1 mM PMSF (Thermo
178 Fisher, # 36978), and homogenized using 10-15 stainless steel beads (0.5 mm
179 diameter, SSB05, Next Advance) in a Bullet Blender tissue homogenizer (Next
180 Advance), speed 8 for 4 minutes and then speed 10 for 2 minutes. The protein
181 lysates were subjected to western blotting using a standard protocol.(9) Samples
182 were separated by sodium dodecyl sulfate-polyacrylamide gel electrophoresis (SDS-
183 PAGE) and then transferred onto a PVDF membrane (Millipore, CA, USA). The
184 following primary antibodies were used: anti-LC3-II (1:3000, Cell Signaling
185 Technology, 12741s) , ubiquitin(1:1000, Invitrogen, #PA5-17067), anti-Atg7(1:1000,
186 Sigma, A2856), anti-Ulk1(1:1000, Cell Signaling Technology, 8054T), anti- β -actin
187 -Peroxidase antibody (1:1000, Sigma, A3854), anti-GAPDH (HRP Conjugate)
188 (1:1000, Cell Signaling Technology, 3683s), anti-Drp1 (1:1000, Cell Signaling
189 Technology, 8750s), anti-Tom20 (1:1000, Cell Signaling Technology, 42406T),
190 mouse anti-rabbit IgG-HRP (1:1000, Santa Cruz Biotechnology, sc-2357).

191 **Measurements of cardiomyocyte size and nuclei size**

192 Fluorescent immunostaining using an anti- β -Catenin (1:200, Sigma, C7207) for the
193 cell membrane and an anti-MEF2(A+C) (1:200, Abcam, ab197070) for
194 cardiomyocyte (CM) nuclei was performed in isolated embryonic zebrafish hearts
195 according to a protocol described previously to measure the CM size and nuclei.(3,
196 16) A Zeiss Axioplan 2 microscope was used for imaging. 15 cells in the outer
197 curvature region (OCR) of each individual heart were selected for measuring the cell
198 surface area using ImageJ software.(3, 17) Only CMs with clear outlines were
199 chosen for the measurement. Measurements from three fishes per group were
200 obtained to calculate the average cardiomyocyte size and nuclei size.

201 **Supplemental tables and figures**202 **Table S1. Genotyping primers.**

Gene	Primer Name	Sequence
<i>ttna-null</i>	ttna-N1F	5'-CGCACCAGTTGTTACTGTC-3'
	ttna-C2R	5'-CATAGTCAGTCTGAACACAAGG-3'
<i>ttnb-null</i>	ttnb-N2F	5'-CAGCAAAAATCACTTTATTCTG-3'
	ttnb-cp-R2	5'-CAAAATGGTGCAGAACTTATGG-3'
<i>ttnd-null</i>	ttna-N1F	5'-CGCACCAGTTGTTACTGTC-3'
	ttnb-cp-R2	5'-CAAAATGGTGCAGAACTTATGG-3'
<i>ulk1a</i>	ulk1a ^{e6} -F	5'-CTGATCCATAACCAATCTGCG-3'
	ulk1a ^{e6} -R	5'-GTCTGAGTGAGGACACCATC-3'
<i>atg7</i>	atg7 ^{e6} -F	5'-GATTGCGTTTCATGTGTCG-3'
	atg7 ^{e6} -R	5'-TCTGCCACAAATGTTACTGATG-3'
<i>anf</i>	Qnppa-F	5'-GATGTACAAGCGCACACGTT-3'
	Qnppa-R	5'-TCTGATGCCTCTTCTGTTGC-3'
<i>bnp</i>	Qnppb-F	5'-CATGGGTGTTTTAAAGTTTCTCC-3'
	Qnppb-R	5'-CTTCAATATTTGCCGCCTTTAC-3'
<i>vmhc</i>	Qvmhc-F	5'-TCAGATGGCAGAGTTTGGAG-3'
	Qvmhc-R	5'-GCTTCCTTTACAGTTACAGTCTTTC-3'
<i>vmhcl</i>	QvmhcL-F	5'-GCGATGCTGAAATGTCTGTT-3'
	QvmhcL-R	5'-CAGTCACAGTCTTGCCCTCCT-3'
<i>ulk1a</i>	Qulk1a ^{e6} -F	5'-CACCATCCGTGTGTTACTGC-3'
	Qulk1a ^{e6} -R	5'-TAGTGTGGCAGCCATTGTGT-3'
	Qulk1a ^{e25} -F	5'-GCTGGCATCAAAGAAGGAAA-3'
	Qulk1a ^{e25} -R	5'-CTGCCGTCTGTACCATCTGA-3'

203

204

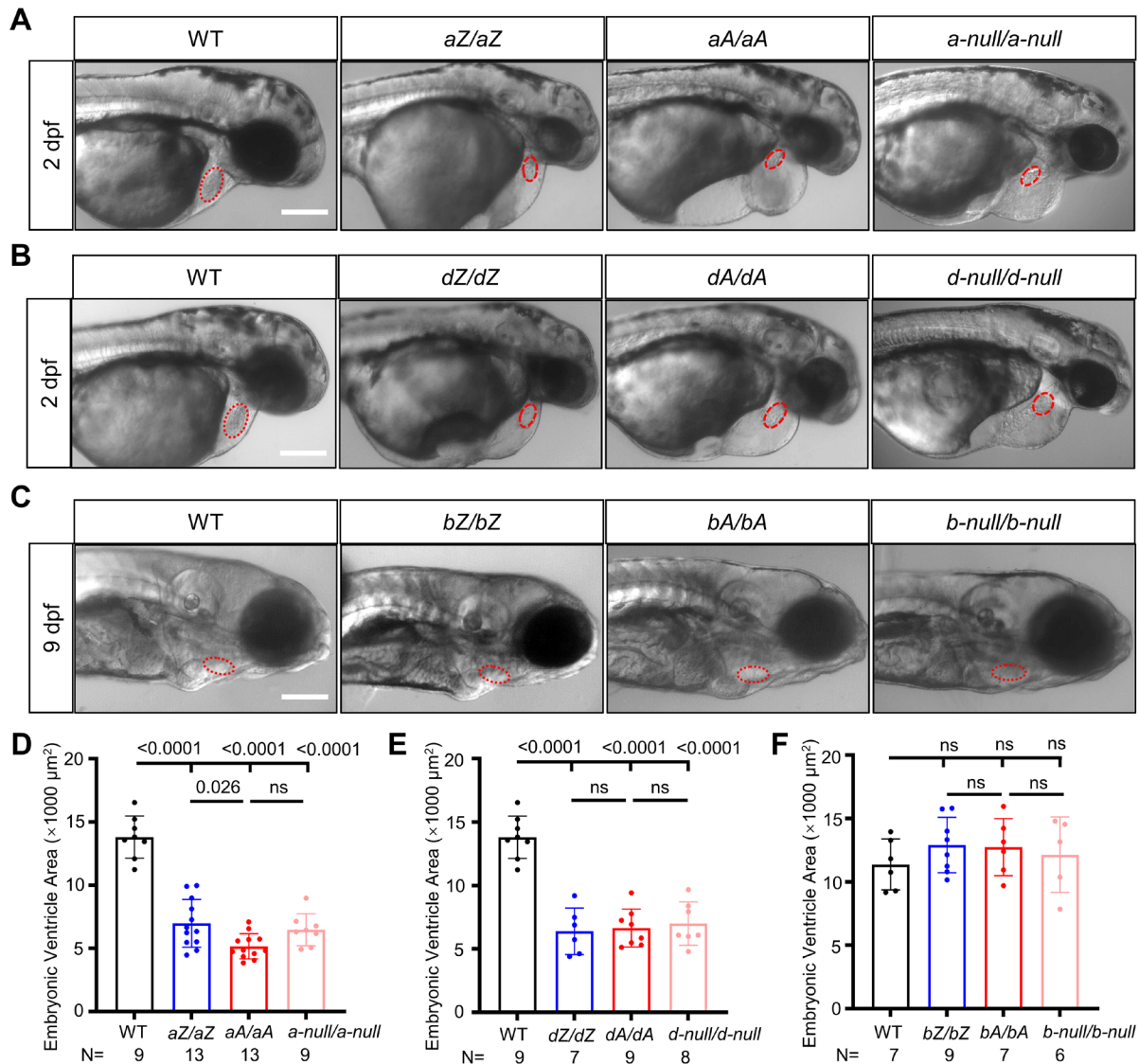
205 **Table S2. Supporting data related to the F0-based MMEJ screen**

Target genes	Design Exon	sgRNA sequence	Frame Shift	Deletion sequence	KO score (%)
<i>atg7</i>	Exon 6	CTGTGCCTCCAGCGGAACGACGG	Yes	AACGACGG	86
<i>ulk1a</i>	Exon 6	ATCCTTCTCTCATACAGCACAGG	Yes	CACAG	92

206

207 **Supplemental movie. Cardiac phenotypes in homozygous *ttntv* embryos**

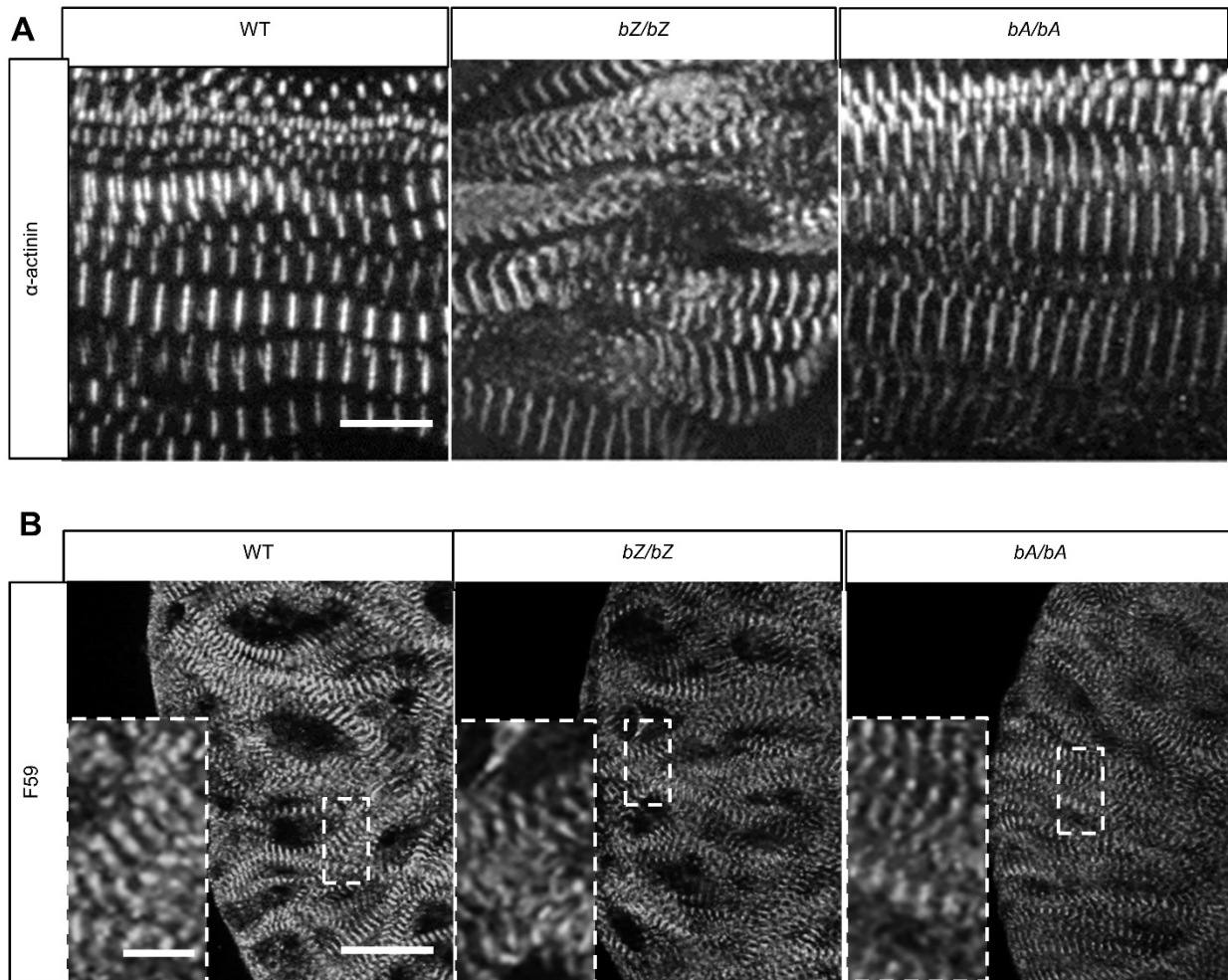
208 Shown are differential interference contrast movies of WT and *ttntv* embryos. Shown
209 in the first two rows are 2 dpf larvae and shown in the bottom row are 9 dpf larvae.
210 60 frames per second.



211
212
213
214
215
216
217
218
219
220
221
222
223
224
225

Figure S1. Pericardiac edema, somite deformation and abnormal ventricle size are detected in *tntv-a* and *tntv-d*, but not in *tntv-b*.

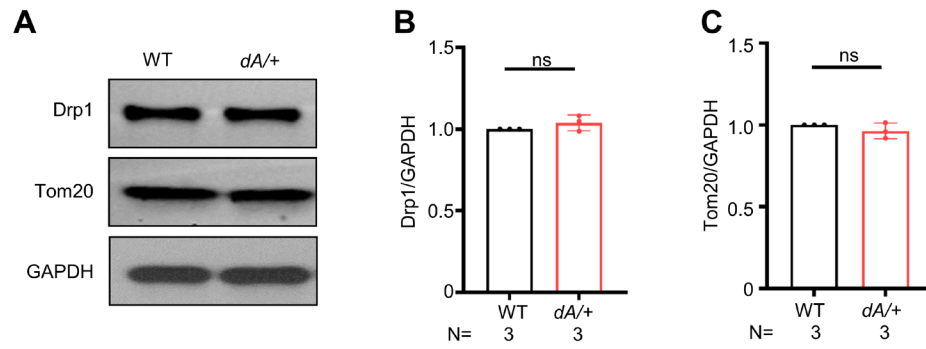
(A-B) Differential interference contrast images of 2 dpf embryos show that the pericardium edema is the common phenotype in all the *TTNtv* mutations but not in WT. Pericardium edema and yolk edema do not belong to a specific mutation. Ventricle size become small, and the heart shape become abnormal in mutation groups, but no difference in each mutation group. (C) Differential interference contrast images of 9 dpf embryos show no pericardium edema, yolk edema, ventricle size, or ventricle shape difference in WT and mutation groups. Scale bar, 200 μm. (D) Quantification of the ventricle area in Figure S1-A. (E) Quantification of the ventricle area in Figure S1-B. (F) Quantification of the ventricle area in Figure S1-C. One-way ANOVA was used to compare multiple groups for each mutation. Data are presented as the mean ± SD. WT, wild type. ns, non-significant.



226

227 **Figure S2. Sarcomere phenotypes in homozygous *bZ* and *bA***

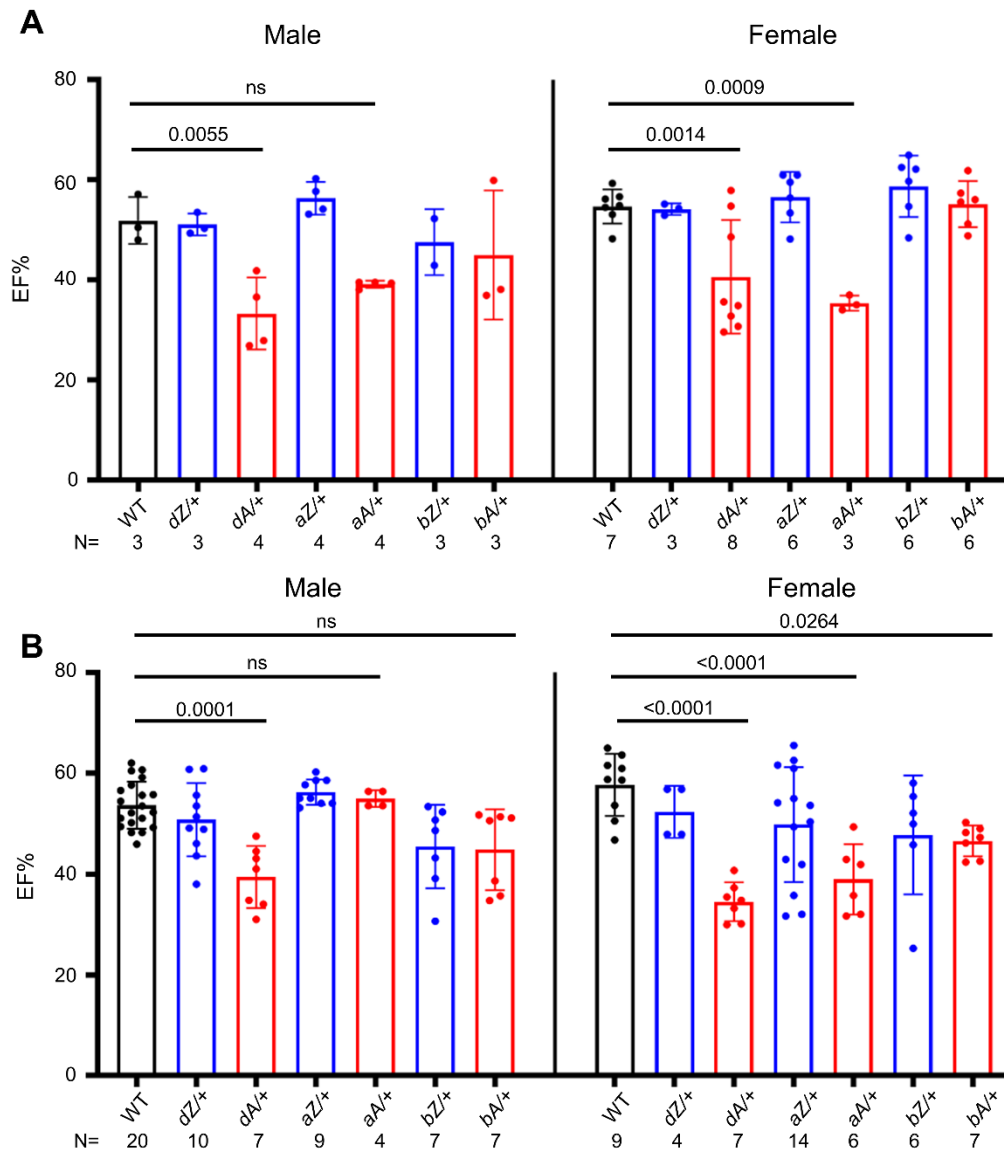
228 (A) Shown are α -actinin antibody immunostaining of the embryonic somites. Similar
 229 to our previous data,(18) *bZ/bZ* but not *bA/bA* and WT exhibits disrupted sarcomere
 230 in somites at 9 dpf. Scale bar= 20 μ m. (B) Shown are F59 antibody immunostaining
 231 of the 9 dpf embryonic heart ventricle. *bZ/bZ* and *bA/bA* do not show significant
 232 difference on sarcomere structure with WT. Scale bar=2 μ m. Insets are enlarged
 233 images of the encircled region. Scale bar=0.5 μ m.



234

235 **Figure S3. Mitochondria dysfunction was not detected at an early stage of**
 236 ***ttnv-A* DCM model.**

237 (A-C) Representative western blot and quantification of Drp1 and Tom20 from
 238 zebrafish hearts at 3 months. Independent samples T-test is applied to compare WT
 239 and *dA/+*. Data are presented as mean ± SD. WT, wild type. ns, non-significant.



240

241 **Figure S4. AH in cardiac dysfunction is more frequently noted in female than**
 242 **male fish**

243 (A) High-frequency echocardiography was performed in fish at 3-month of age.

244 Female *dA/+* and *aA/+* fish manifest severer cardiac dysfunction than male fish. (B)

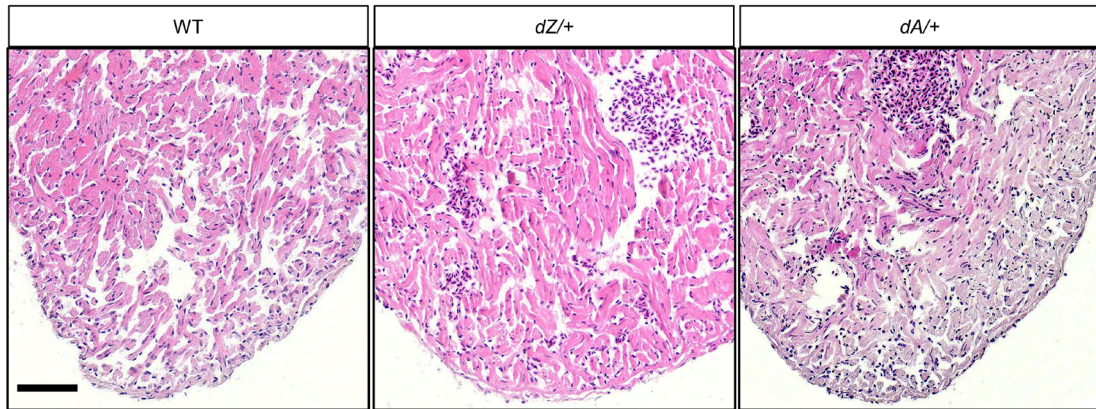
245 High-frequency echocardiography was performed at 6-month of age. Female *dA/+*,

246 *aA/+* and *bA/+* fish show more markedly reduction of EF than male fish. One-way

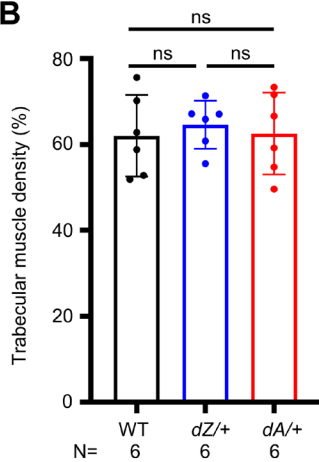
247 ANOVA was used to compare multiple groups for each mutation. Data are presented

248 as mean \pm SD. WT, wild type. ns, non-significant.

A



B

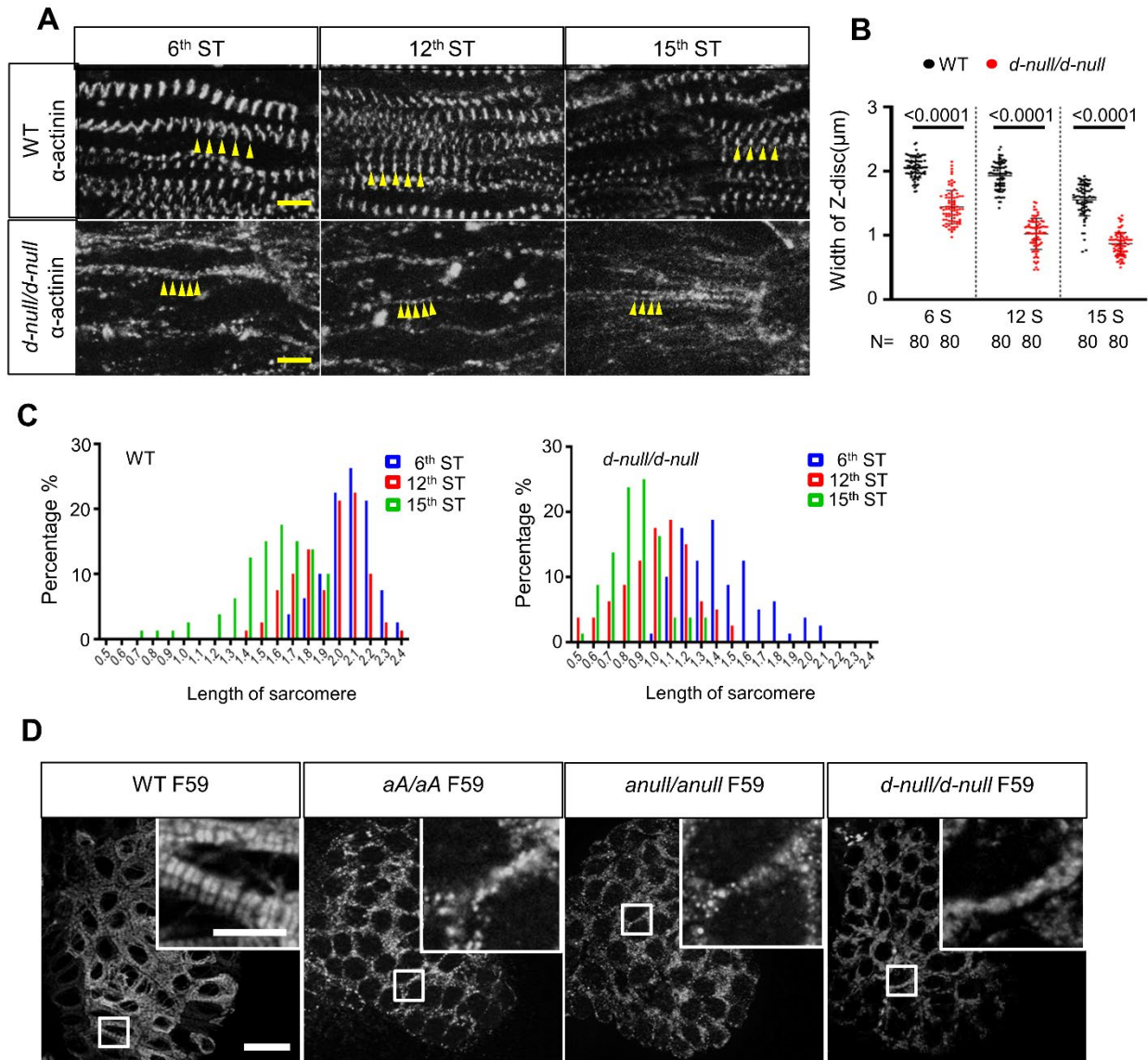


249

250 **Figure S5. Trabecular muscle density was unchanged in the *ttntv***
251 **heterozygous fish.**

252 (A-B) Representative images of H&E staining in the apex area of ventricle and
253 quantification of trabecular muscle density in fish at 3 months. Scale bar =50 μ m.
254 One-way ANOVA was used to compare multiple groups for each mutation. Data are
255 presented as the mean \pm SD. WT, wild type. ns, non-significant.

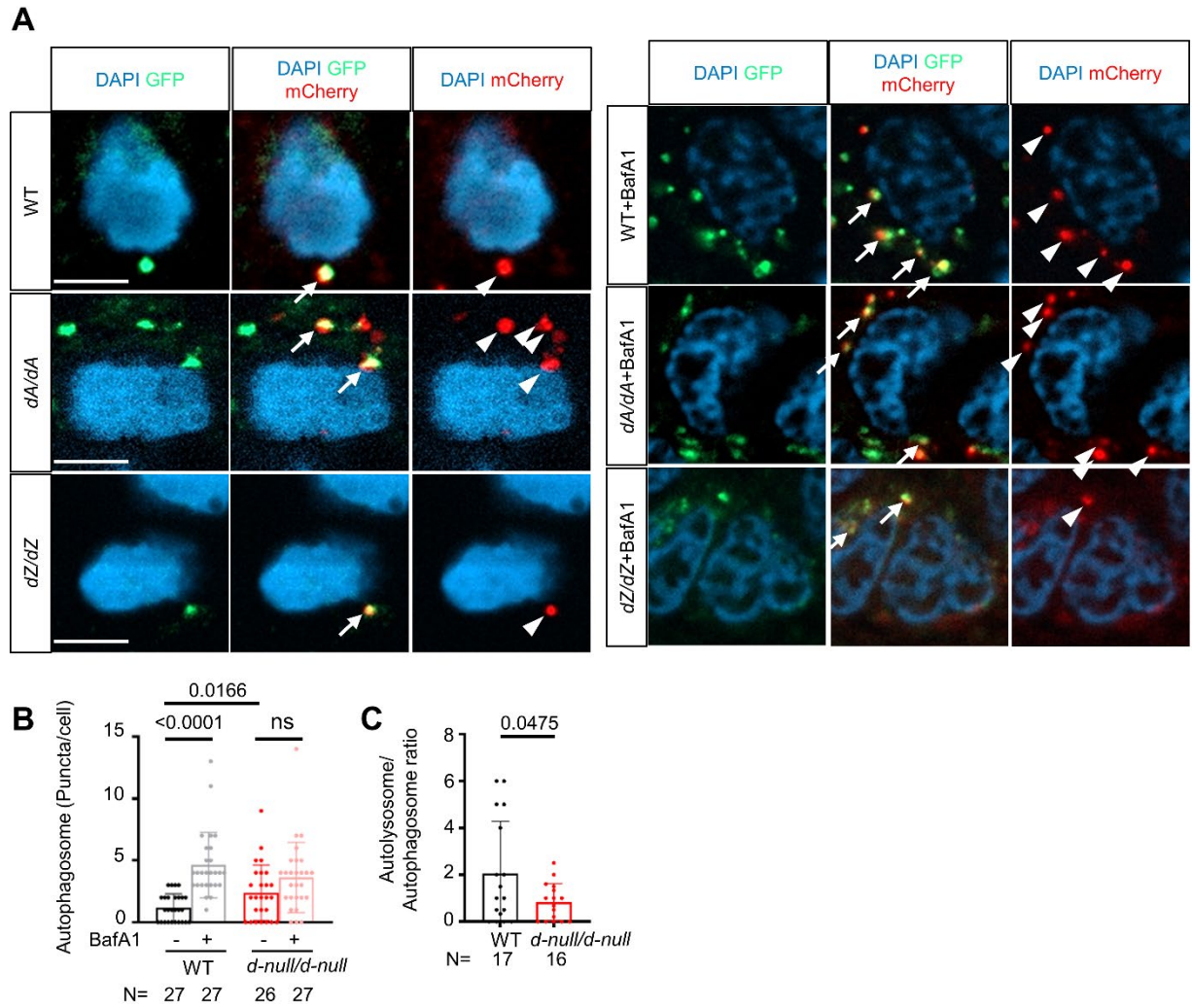
256



257

258 **Figure S6. *d-null/d-null* manifests sarcomeric defects**

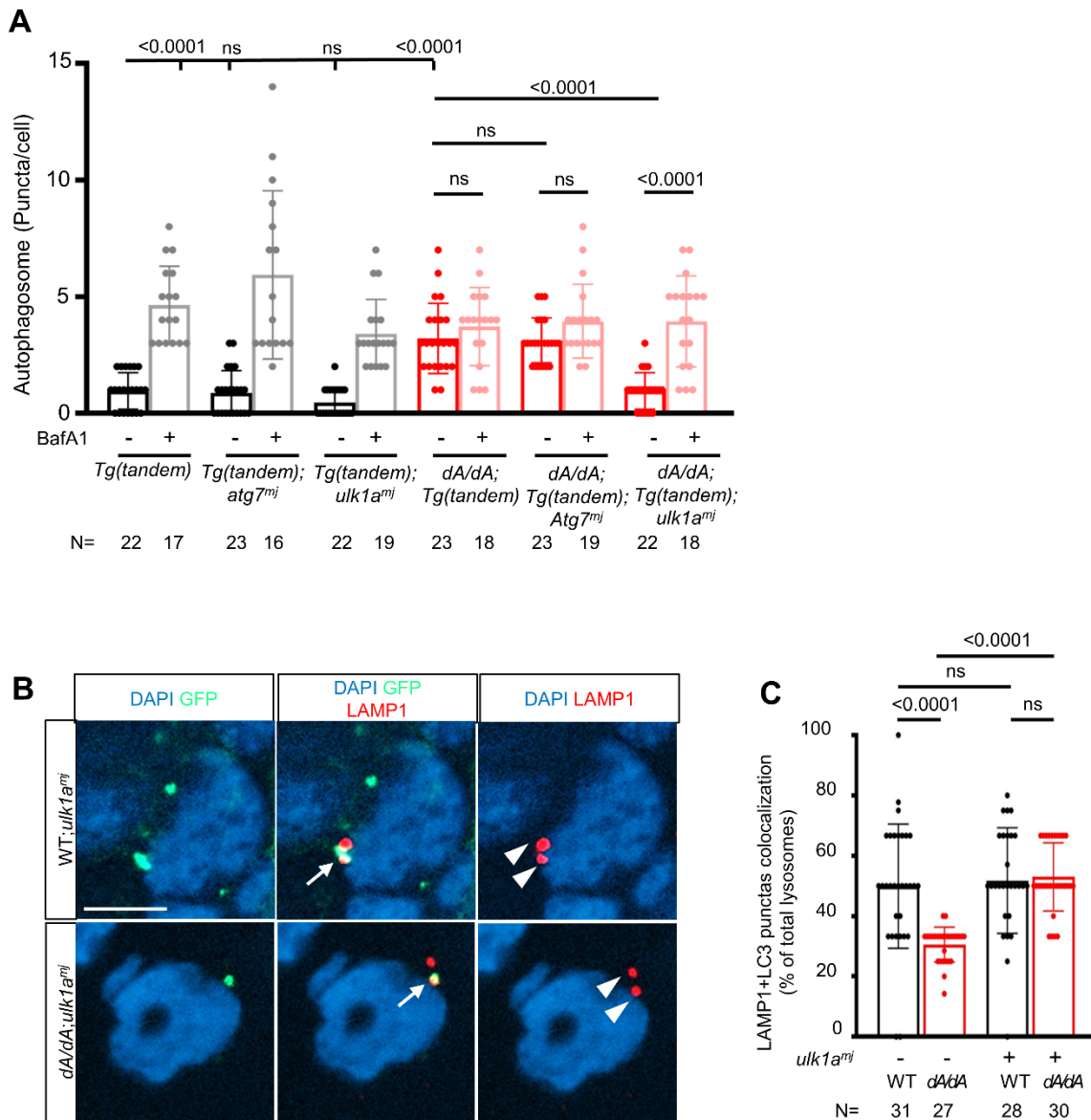
259 (A) Shown are anti- α -actinin immunostaining of WT and *d-null/d-null* mutant embryos
 260 at the 18-somite (ST) stage. Images were captured at the 6th, 12th and 15th somites,
 261 respectively, representing three different stages of myofibrillogenesis. Yellow
 262 arrowheads indicate the striated sarcomere. Scale bar= 5 μ m. (B) Quantification of
 263 width of the Z-discs of WT and *d-null/d-null* mutant at the 6th, 12th and 15th somites.
 264 Independent samples T-test is applied to compare the difference between WT and *d-*
 265 *null/d-null*. Data are presented as mean \pm SD. WT, wild type. (C) Frequency
 266 distributions of length of sarcomere in 6th, 12th, and 15th somites of WT and *d-null/d-*
 267 *null*, as measured by the distance between neighboring two yellow arrowheads in
 268 panel A. n=80 for each group in different somites. (D) Comparison of cardiac
 269 sarcomere structure in 2 dpf embryos via F59 antibody staining. Scale bar=10 μ m.
 270 Insets show enlarged images of the area circled with dashed lines. Scale bar=5 μ m.



271

272 **Figure S7. Additional data for Figure 5.**

273 (A) Representative images of a cardiomyocyte in a embryonic heart injected with a
 274 *mCherry-EGFP-LC3II* tandem plasmid. The arrow indicates a yellow puncta with
 275 both GFP and mCherry that presumably represents an autophagosome, and the
 276 arrowhead indicates a red puncta with mCherry that presumably represents an
 277 autolysosome. Scale bar: 5 μ m. (B) Autophagy regulation in *d-null/d-null* embryos.
 278 Quantification of the autophagosome puncta in 2-dpf *d-null/d-null* embryos with
 279 BafA1 treatment. One-way ANOVA was used to compare multiple groups. (C) The
 280 autolysosome/autophagosome ratio in 2-dpf *d-null/d-null* embryos without BafA1-
 281 treatment. Independent samples T-test is applied. Data are presented as mean \pm
 282 SD. WT, wild type. ns, non-significant.



283

284

285

Figure S8. An F0-based MMEJ assessment of candidate genes related to autophagy regulation in *ttntv-A* and the fusion-rescuing effects of *ulk1a*.

286

287

288

289

290

291

292

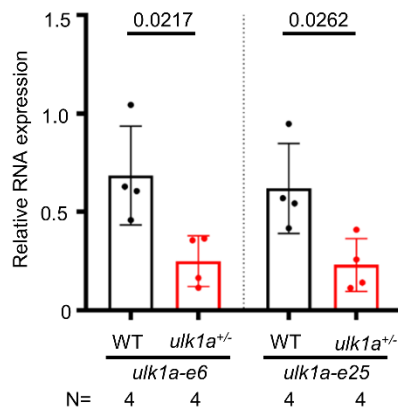
293

294

295

296

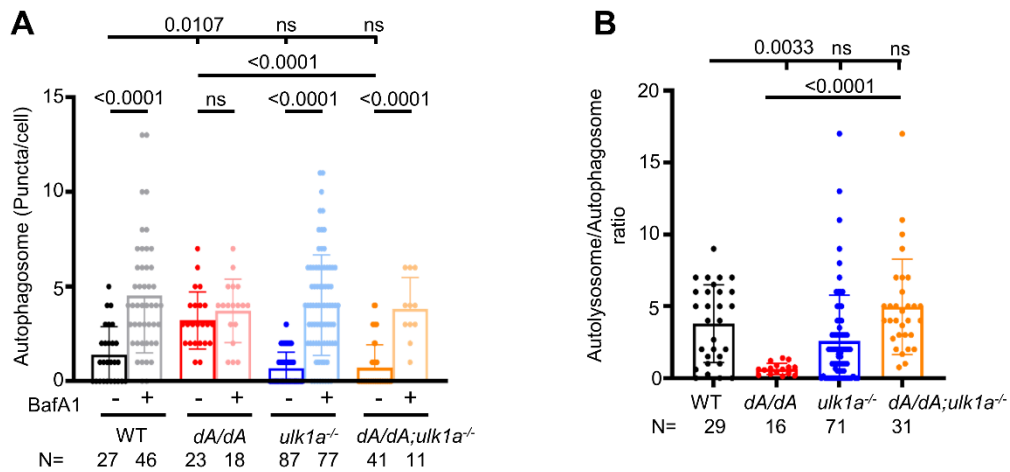
(A) Quantification of autophagosome puncta in zebrafish embryos co-injected with *mCherry-EGFP-LC3II* tandem plasmid and sgRNAs against autophagy genes. *ulk1a^{mj}* but not *atg7^{mj}* rescued autophagy dysregulation by reducing the basal level of autophagy and increasing autophagic flux. (B) Representative image and quantification of LC3-GFP and lysosome marker LAMP1 colocalization compared with the total lysosome. The arrow indicates a yellow puncta with both GFP and LAMP1 that represents co-localization, and the arrowhead indicates a red puncta with only LAMP1. Scale bar: 5 μ m. (C) Quantification of (B), depletion of *ulk1a* rescues the impairment of autophagosome-lysosome fusion in *dA/dA* hearts. One-way ANOVA was used to compare multiple groups. Data are presented as the mean \pm SD. WT, wild type. ns, non-significant.



297

298 **Figure S9. Expression levels of *ulk1a* transcripts**

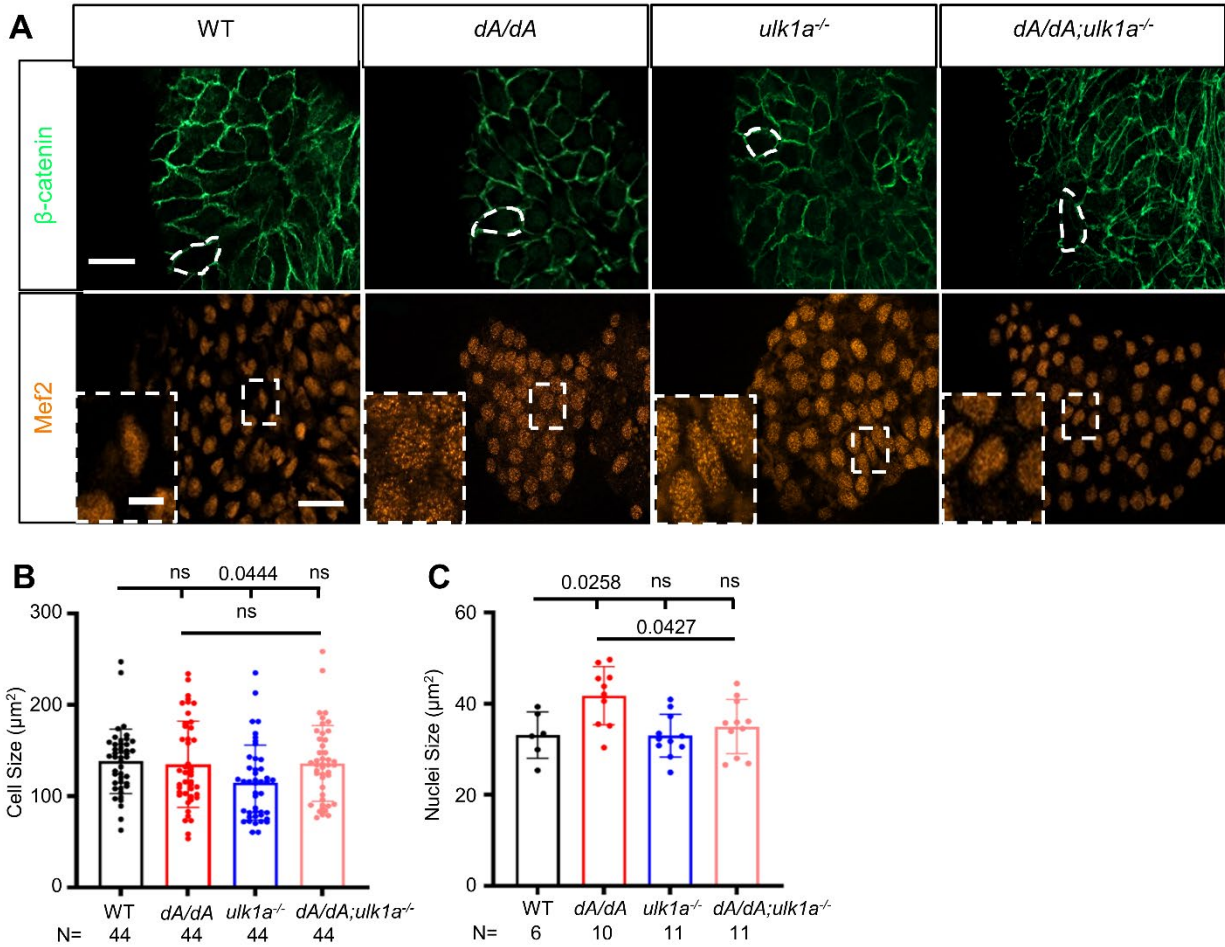
299 Transcripts of *ulk1a* are reduced in *ulk1a*^{+/-}. The expression levels of *ulk1a*
 300 transcripts were measured by quantitative RT–PCR. Primer pairs are located in exon
 301 6 and exon 25 of *ulk1a*. Independent samples T-test is applied to compare the
 302 difference between WT and *ulk1a*^{+/-}. Data are presented as mean ± SD. WT, wild
 303 type.



304

305 **Figure S10. *ulk1a* homozygous mutant repairs autophagy dysregulation in**
 306 **embryonic stage *ttntv* mutants**

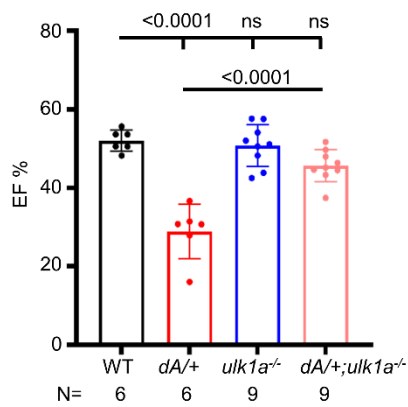
307 (A) Quantification of the autophagosome puncta in 2-dpf embryos either with or
 308 without BafA1 treatment. (B) The autolysosome/autophagosome ratio of BafA1
 309 untreated groups. *ulk1a^{-/-}* can reduce the basal autophagosome level of *dA/dA* and
 310 can recover the autophagic flux affected by *dA/dA*. One-way ANOVA was used to
 311 compare multiple groups for each mutation. Data are presented as mean ± SD. WT,
 312 wild type. ns, non-significant.



313

314 **Figure S11. *ulk1a* mutant attenuates the enlarged nuclear size in *dA/dA***
 315 **ventricles**

316 (A) Representative images of hearts from 2-dpf embryos after immunostaining. The
 317 nucleus and membrane of cardiomyocytes (CMs) were identified by immunostaining
 318 with anti-myocyte enhancer factor-2 (Mef2) (orange) and anti- β -catenin (green)
 319 antibodies, respectively. Representative CMs in the outer curvature are outlined by
 320 the dashed white lines. Insets are higher magnification images of the boxed areas.
 321 Scale bar = 10 μm . Scale bar in insets is 2.5 μm . (B) Quantification of the CM cell
 322 area based on anti- β -catenin staining. (C) Quantification of the nuclear area based
 323 on anti-Mef2 staining. One-way ANOVA was used to compare multiple groups for
 324 each mutation. Data are presented as the mean \pm SD. WT, wild type. ns, non-
 325 significant.



326

327 **Figure S12. *ulk1a* homozygous mutant repairs cardiac dysfunction in *tntv-A***
 328 **adult fish.**

329 High-frequency echocardiography was performed on 3-month-old zebrafish to
 330 quantify EF%. One-way ANOVA was used to compare multiple groups for each
 331 mutation. Data are presented as mean \pm SD. WT, wild type. ns, non-significant.

332

333 **Supplemental references**

- 334 1. Asquith B, and Bangham CR. An introduction to lymphocyte and viral dynamics:
335 the power and limitations of mathematical analysis. *Proc Biol Sci.*
336 2003;270(1525):1651-7.
- 337 2. Hoage T, Ding Y, and Xu X. Quantifying cardiac functions in embryonic and
338 adult zebrafish. *Methods Mol Biol.* 2012;843:11-20.
- 339 3. Yang JC, and Xu XL. Immunostaining of Dissected Zebrafish Embryonic Heart.
340 *Jove-J Vis Exp.* 2012(59).
- 341 4. Wang LW, Huttner IG, Santiago CF, Kesteven SH, Yu ZY, Feneley MP, et al.
342 Standardized echocardiographic assessment of cardiac function in normal
343 adult zebrafish and heart disease models. *Dis Model Mech.* 2017;10(1):63-76.
- 344 5. Zhang H, Dvornikov AV, Huttner IG, Ma X, Santiago CF, Fatkin D, et al. A
345 Langendorff-like system to quantify cardiac pump function in adult zebrafish.
346 *Dis Model Mech.* 2018;11(9).
- 347 6. Ma X, and Xu X. A Swimming-based Assay to Determine the Exercise Capacity
348 of Adult Zebrafish Cardiomyopathy Models. *Bio Protoc.* 2021;11(15):e4114.
- 349 7. Sun YY, Fang YH, Xu XL, Lu GP, and Chen ZY. Evidence of an Association
350 between Age-Related Functional Modifications and Pathophysiological
351 Changes in Zebrafish Heart. *Gerontology.* 2015;61(5):435-47.
- 352 8. Wang JH, Panakova D, Kikuchi K, Holdway JE, Gemberling M, Burris JS, et al.
353 The regenerative capacity of zebrafish reverses cardiac failure caused by
354 genetic cardiomyocyte depletion. *Development.* 2011;138(16):3421-30.

- 355 9. Ding Y, Dvornikov AV, Ma X, Zhang H, Wang Y, Lowerison M, et al.
356 Haploinsufficiency of mechanistic target of rapamycin ameliorates bag3
357 cardiomyopathy in adult zebrafish. *Dis Model Mech.* 2019;12(10).
- 358 10. Chung K, Wallace J, Kim SY, Kalyanasundaram S, Andalman AS, Davidson TJ,
359 et al. Structural and molecular interrogation of intact biological systems. *Nature.*
360 2013;497(7449):332-+.
- 361 11. Bu H, Ding Y, Li J, Zhu P, Shih YH, Wang M, et al. Inhibition of mTOR or MAPK
362 ameliorates vmhcl/myh7 cardiomyopathy in zebrafish. *JCI Insight.* 2021;6(24).
- 363 12. Truett GE, Heeger P, Mynatt RL, Truett AA, Walker JA, and Warman ML.
364 Preparation of PCR-quality mouse genomic DNA with hot sodium hydroxide
365 and tris (HotSHOT). *Biotechniques.* 2000;29(1):52, 4.
- 366 13. Brinkman EK, and van Steensel B. Rapid Quantitative Evaluation of CRISPR
367 Genome Editing by TIDE and TIDER. *Methods Mol Biol.* 2019;1961:29-44.
- 368 14. Bhattacharya D, and Van Meir EG. A simple genotyping method to detect small
369 CRISPR-Cas9 induced indels by agarose gel electrophoresis. *Sci Rep.*
370 2019;9(1):4437.
- 371 15. Warren CM, Krzesinski PR, and Greaser ML. Vertical agarose gel
372 electrophoresis and electroblotting of high-molecular-weight proteins.
373 *Electrophoresis.* 2003;24(11):1695-702.
- 374 16. Yang JC, Hartjes KA, Nelson TJ, and Xu XL. Cessation of contraction induces
375 cardiomyocyte remodeling during zebrafish cardiogenesis. *Am J Physiol-Heart*
376 *C.* 2014;306(3):H382-H95.

- 377 17. Auman HJ, Coleman H, Riley HE, Olale F, Tsai HJ, and Yelon D. Functional
378 modulation of cardiac form through regionally confined cell shape changes.
379 *Plos Biol.* 2007;5(3):604-15.
- 380 18. Shih YH, Dvornikov AV, Zhu P, Ma X, Kim M, Ding Y, et al. Exon- and
381 contraction-dependent functions of titin in sarcomere assembly. *Development.*
382 2016;143(24):4713-22.
- 383